Monograph:
Guo, L.Z. and Billings, S.A. (2004) Identification of Coupled Map Lattice Models of Stochastic Spatio-Temporal Dynamics Using Wavelets. Research Report. ACSE Research Report 851 . Department of Automatic Control and Systems Engineering

eprints@whiterose.ac.uk
https://eprints.whiterose.ac.uk/

IDENTIFICATION OF COUPLED MAP LATTICE MODELS OF STOCHASTIC SPATIO-TEMPORAL DYNAMICS USING WAVELETS

L. Z. GUO AND S. A. BILLINGS

Department of Automatic Control and Systems Engineering
University of Sheffield
Sheffield, S1 3JD
UK

Identification of coupled map lattice models of stochastic spatio-temporal dynamics using wavelets

Guo, L. Z. and Billings, S. A.

Department of Automatic Control and Systems Engineering
University of Sheffield
Sheffield S1 3JD, UK

Abstract

This paper introduces a new approach for the local reconstruction of coupled map lattice (CML) models of stochastic spatio-temporal dynamics from measured data. The nonlinear functionals describing the evolution of the spatio-temporal patterns are constructed using B-spline wavelet and scaling functions. This provides a multiresolution approximation for the underlying spatio-temporal dynamics. An orthogonal least squares algorithm is used to determine significant terms from wavelet functions to form an accurate representation of the nonlinear spatio-temporal dynamics. Two examples are used to demonstrate the application of the proposed new approach.

1 Introduction

Complex spatio-temporal patterns have been widely observed and explored in many diverse fields including physical, chemical, biological, and ecological systems (Kaneko 1993, Sóle, Valls and Bascompte 1992, Yanagita and Kaneko 1997, Tabuchi, Yakawa and Mallick et al. 2002, Köhler, Reinhard and Huth 2002, Bertram, Beta, Rotermund, and Ertl 2003, Goldman, et al. 2003, Adamatzky 2003). Coupled map lattices (CML) have been studied in recent years as an effective model of spatio-temporal dynamical systems. Among these studies, various methods for the identification of local CML models from spatio-temporal observations have been proposed (Coca and Billings 2001, Mandelj, Grabec and Govekar 2001, Marcos-Nikolaus, Martin-Gonzalez and Sóle 2002, Grabec and Mandeji 1997, Parlitz and Merkwirth 2000, Coca and billings, 2003, Gradisek, Siegert, Friedrich, and Grabec 2000, Blanc-Talon 1999, Billings, Wei, Mei, and Guo 2003, Billings, Guo, and Wei 2003). Because in practice all physical systems are, to some extent, subject to stochastic noise or perturbations either due to measurement errors or unknown disturbances, it is important to develop models and identification procedures which can accommodate

stochastic effects. However, there are very few results for the identification or reconstruction problem of stochastic spatio-temporal dynamical systems. The aim of this paper is to present a systematic methodology to reconstruct CML equations from noise-corrupted measured data using wavelets as regressors.

Theoretical studies have shown that the wavelet representation of any nonlinear function can be shown to be asymptotically near optimal in the sense that the convergence rates are equal to the best attainable using general nonlinear approximation schemes (DeVore, Jawerth, and Popov 1992). In addition wavelet approximations also provide similar rates of approximation for functions belonging to a wide variety of function spaces including functions with sparse singularities or functions that are not uniformly smooth or regular. Finally, wavelets allow localisation in both time and frequency, which means that the approximation can be refined locally over a subregion in the input domain without affecting the model elsewhere too much. All these properties suggest that wavelet multiresolution expansions should provide an excellent foundation for the development of identification algorithms for nonlinear CML models.

In this paper, wavelets, as regressors, are used to identify the CML models, which drive spatio-temporal pattern formation, from noisy data for the purpose of revealing the dynamical origin of the given patterns. The nonlinear functionals describing the evolution of the spatio-temporal patterns are constructed using B-spline wavelet and scaling functions, originally introduced by Chui and Wang (1991). The forward regression orthogonal least squares algorithm proposed by Chen, Billings, and Luo (1989) is used to determine the most significant terms from the B-spline wavelet and scaling functions. The paper is organised as follows. Section 2 introduces the CML model of stochastic spatio-temporal dynamical systems. The wavelet models are introduced in section 3 including an introduction to wavelets and a discussion about wavelet model structures. In section 4, the identification method and the implementation strategy are presented. Section 5 illustrates the proposed approach using two examples. Finally conclusions are drawn in section 6.

2   A CML model for stochastic spatio-temporal systems

Stochastic spatio-temporal dynamical systems are stochastic processes whose evolution is indexed by both time and spatial parameters. The behaviour of such systems can be statistically described by the evolution of the probability density functions. The stochastic spatio-temporal systems studied in this paper are those that can be modelled by the following CML defined on a discrete lattice I

$$\mathbf{x}(t) = \mathbf{F}(\mathbf{x}(t-1), \mathbf{u}(t-1), \mathbf{e}(t)) \tag{1}$$

where $\mathbf{x}(t) \in X$ and $\mathbf{u}(t) \in U$ are the state and external input at time instant t, respectively. $\mathbf{F}$ is a nonlinear map. $\mathbf{e}(t) \in E$ is a random vector representing the internal noise perturbation defined on I. Specifically, the evolution of each site i in I of the CML equation (1) is given by

$$x_i(t) = F_i(x_i(t-1), u_i(t-1), e_i(t), \nabla_i(t)), i \in I \tag{2}$$

where $\nabla_i(t)$ indicates all coupling effects for site i at time instant t from the spatial neighbourhood sites in $\Omega \subset I$ which involves $x_j(t-1), u_j(t-1), e_j(t-1), j \in \Omega$. The spatial neighbourhood Ω of a specified site is the region around that site which influences the dynamics of that site.

Clearly, the dimension of the state space depends on the size of the lattice I. In general, the dimension will be infinite-dimensional if the number of elements of the lattice is infinite. For the local reconstruction problem, it is sufficient to consider the dimension as being finite dimensional with dimension n. In this case, the internal noise perturbation $\mathbf{e}(t)$ is a n-dimensional random vector whose components are assumed to be independent, each described by a one-dimensional probability density ϕ.

Let $p(\mathbf{x}(t)|\mathbf{x}(t-1), \mathbf{u}(t-1)))$ be the conditional probability density function of the state $\mathbf{x}(t)$ of (1). This conditional density function for $t = 1, 2, \cdots$ specifies a causal stochastic system completely. Therefore, the stochastic dynamics of the underlying system can be completely determined if the conditional probability density function can be obtained exactly at each time instant. Generally, the statistical behaviour of the system (1) can be exploited by studying the evolution of the conditional probability density using transfer operators if this is known or the density function can be estimated. For example, if the system (1) takes the form of a Langevin equation, then the evolution of the probability density distribution p can be described using the Fokker-Planck equation. The stochastic dynamics of the Langevin equation can be reconstructed in terms of the drift and diffusion coefficients of the Fokker-Planck equation (Gradisek, Siegert, Friedrich, and Grabec 2000). The performance of the reconstruction depends on the accuracy of the estimated drift and diffusion coefficients. For more general stochastic dynamics, the Frobenius-Perron operator can be used to describe the evolution of the probability density distributions (Losson and Mackey 1995, Coca and Billing 2003). Using the Frobenius-Perron operator or transfer operator, the statistical behaviour of the system can be studied qualitatively. In this paper, instead of using the transfer operator to study and analyse the statistical behaviour, the reconstruction problem of the local stochastic dynamics from measured spatio-temporal data will be addressed using wavelets.

Before proceeding to the reconstruction algorithm, consider the derivation of an input-output representation of the CML (1), which will be used as a basis for the reconstruction. Assume that the state-space model of the CML is complemented with the following measurement equation

$$y_i(t) = h_i(\mathbf{x}(t)) \tag{3}$$

It is assumed that the lattice equations are spatially invariant over the observed spatial domain. This implies that the difference equations corresponding to each lattice site or location are the same for all lattice sites. Generally it is also assumed that the following input-output representation

3

$$y_i(t) = f(y_i(t-1), \cdots, y_i(t-n_y); u_i(t), \cdots, u_i(t-n_u); e_i(t), \cdots, e_i(t-n_e); \nabla_i(t), \cdots, \nabla_i(t-n_c)) \tag{4}$$

can be derived for any site i from (2) and (3).

From eqn.(4), it can be seen that the input-output dynamics of the model can be affected by the noise perturbations from adjacent lattice sites. Because the noise $e_i(t)$ is not measurable at time instant t, it is assumed that the model (4) can always be represented in the prediction error form

$$y_i(t) = f(y_i(t-1), \cdots, y_i(t-n_y); u_i(t), \cdots, u_i(t-n_u); e_i(t-1), \cdots, e_i(t-n_e); \nabla_i(t), \cdots, \nabla_i(t-n_c)) + e_i(t) \tag{5}$$

where there are no coupling noise effects from other sites and $e_i(t)$ enters the model linearly. In practice, eqn.(5) can be used to represent a wide class of stochastic spatio-temporal dynamical systems. In what follows, multivariate wavelets are chosen as basis functions to approximate the CML model (5).

3 Multivariate wavelets for CML identification

The task of CML identification is to reproduce the spatio-temporal relation f, which is essentially multivariate and nonlinear, in eqn. (5) from measured noisy data. This objective is complex when f is nonlinear. The most commonly used approach to finding approximations to unknown functions is to generate a best approximation from a given class of approximation functions. The general requirement for the class of approximation functions is that they are relatively smooth and easy to process on a digital computer. In this paper, a class of approximation functions generated by multivariate wavelets will be applied to approximate the nonlinear function f.

The wavelet decomposition of a multivariate function f defined on R^n can be described as follows. Let Φ be a bounded function defined on R^n. For all $j \in Z$ and $k \in Z^n$, a series of functions defined on R^n can be derived in terms of the translates and dyadic dilates of Φ: $\Phi(2^j \mathbf{x} - k)$. Then if $\Phi_{j,k}(\mathbf{x}) = \Phi(2^j \mathbf{x} - k)$, $j \in Z, k \in Z^n$ form a Riesz basis, function f has a decomposition in terms of $\Phi_{j,k}(\mathbf{x}) = \Phi(2^j \mathbf{x} - k)$, $j \in Z, k \in Z^n$

$$f(\mathbf{x}) = \sum_j \sum_k a_{j,k} \Phi_{j,k}(\mathbf{x}) \tag{6}$$

Such a Riesz basis in space $L^2(R^n)$ can be constructed from the univariate scaling function ϕ and the associated wavelet function ψ by using the tensor product method. Assuming $\mathbf{x} = \{x_1, x_2\}$ for example, define

4

$$\Psi^{(0)}(\mathbf{x}) = \phi(x_1)\phi(x_2); \Psi^{(1)}(\mathbf{x}) = \phi(x_1)\psi(x_2); \Psi^{(2)}(\mathbf{x}) = \psi(x_1)\phi(x_2); \Psi^{(3)}(\mathbf{x}) = \psi(x_1)\psi(x_2) \quad (7)$$

By translates and dyadic dilates the set of functions given in (7) generates a Riesz basis in $L^2(R^2)$. This means the each function $f \in L^2(R^2)$ has the following unique decomposition

$$f(\mathbf{x}) = \sum_{j,k,l} a_{j,k}^{(l)} \Psi_{j,k}^{(l)}(\mathbf{x}) \quad (8)$$

where $\Psi_{j,k}^{(l)}(\mathbf{x}) = 2^{j/2}\Psi^{(l)}(2^j\mathbf{x} - k)$, $j \in Z, k \in Z^n$.

The univariate scaling function considered in this paper is the m-th order cardinal B-spline function $\phi(x) = \phi^m(x) = \beta^m(x)$ given by the recursive relation

$$\beta^m(x) = \frac{x}{m-1}\beta^{m-1}(x) + \frac{m-x}{m-1}\beta^{m-1}(x-1) \quad (9)$$

where $\beta^1(x)$ is the indicator function

$$\beta^1(x) = \{ \begin{array}{ll} 1 & \text{if } x \in (0,1) \\ 0 & \text{otherwise} \end{array} \quad (10)$$

The wavelet function is defined as a linear combination of scaling functions

$$\psi^m(x) = \sum_{l=0}^{3m-2} q_l \phi^m(2x - l) \quad (11)$$

with the coefficients given by

$$q_l = \frac{(-1)^l}{2^{m-1}} \sum_{k=0}^{m} \binom{m}{k} \phi^{2m}(l-k+1), \ l = 0, \cdots .3m - 2 \quad (12)$$

Assume that the nonlinear multivariate function f in eqn. (5) is in $L^2(R^n)$. Then the B-spline wavelet representation of the input-output CML equation (5) can be described as follows

$$y_i(t) = f(\mathbf{x}) + e_i(t) = \sum_{j,k,l} \theta_{j,k,l} \Psi_{j,k}^{(l)}(\mathbf{x}) + e_i(t), j \in Z, k \in Z^n, l = 1, \cdots, 2^n - 1 \quad (13)$$

where

5

$$\mathbf{x} = (y_i(t-1), \cdots, y_i(t-n_y); u_i(t), \cdots, u_i(t-n_u); e_i(t-1), \cdots, e_i(t-n_e); \nabla_i(t), \cdots, \nabla_i(t-n_c))^T \tag{14}$$

as shown in eqn. (5).

According to the multiresolution analysis, eqn. (13) can equivalently be expressed as

$$y_i(t) = f(\mathbf{x}) + e_i(t) = \sum_{j \leq j_0, k} \theta_{j,k,0} \Psi_{j,k}^{(0)}(\mathbf{x}) + \sum_{j \geq j_0, k, l} \theta_{j,k,l} \Psi_{j,k}^{(l)}(\mathbf{x}) + e_i(t), k \in Z^n, l = 1, \cdots, 2^n - 1 \tag{15}$$

4   Identification algorithm

In theory, the wavelet multiresolution approximation is an infinite series expansion. In practice, however, it is not realistic to use all the terms in this infinite series expansion. Generally the objective of the identification algorithm is to obtain a truncated finite representation containing the terms up to some orders of scaling and dilation. Therefore the identified CML model will be an approximate representation of the underlying spatio-temporal dynamics, which can be equivalently described as an infinite wavelet series. Although this is a finite approximation representation, in practice, it can be made to approximate the underlying dynamics at any given accuracy. Let $s > 0$ be an integer, the s-truncated space Σ_{s,j_0} with a starting resolution j_0 is the set of all functions

$$f(\mathbf{x}) = \sum_{j \leq j_0, k} \theta_{j,k,0} \Psi_{j,k}^{(0)}(\mathbf{x}) + \sum_{j_0 \leq j \leq s, k, l} \theta_{j,k,l} \Psi_{j,k}^{(l)}(\mathbf{x}), k \in Z^n, l = 1, \cdots, 2^n - 1 \tag{16}$$

In this paper, Σ_{s,j_0} is considered as the approximation space for the identification of CML models. Note that the series in space Σ_{s,j_0} are those up to dyadic level s, which may possibly be infinite because there is no limitation on the translation operation. In practice, the range of measured data is always finite so that there are only finite numbers of translation operations which produce non-empty intersections with the range of data. Therefore, the identified wavelet series are always finite. Furthermore, in many applications, a 3-truncated space is often enough to obtain a good approximation result because the wavelets with higher dyadic level are most likely to have compact support which contains no data points.

Unlike the deterministic case the identification of a CML model for stochastic spatio-temporal systems involves dealing with stochastic perturbations. Since in practice the noise perturbations cannot be measured, the unobserved noise sequence has to be estimated from the identification data using a prediction error approach. The prediction error can be calculated by the following formulation with the approximation space Σ_{s,j_0}

6

$$\varepsilon_i(t) = y_i(t) - \hat{y}_i(t) = y_i(t) - \left(\sum_{j \leq j_0, k} \theta_{j,k,0} \Psi_{j,k}^{(0)}(\mathbf{x}) + \sum_{j_0 \leq j \leq s, k, l} \theta_{j,k,l} \Psi_{j,k}^{(l)}(\mathbf{x}) \right) \tag{17}$$

where

$$\mathbf{x} = (y_i(t-1), \cdots, y_i(t-n_y); u_i(t), \cdots, u_i(t-n_u); \varepsilon_i(t-1), \cdots, \varepsilon_i(t-n_e); \nabla_i(t), \cdots, \nabla_i(t-n_c))^T \tag{18}$$

If ε_i is zero mean and white then the estimates will be unbiased.

A key task of the identification algorithm is to be able to select the significant model terms for the final representation from a given set of candidate terms $\{\Psi_{j,k}^{(l)}(\mathbf{x})\}, j \leq s \in Z, k \in Z^n$, and $l = 0, \cdots, 2^n - 1$ such that $\varepsilon_i(t)$ tends to $e_i(t)$ as $t \to \infty$. In this paper, a forward regression orthogonal least squares algorithm (Chen, Billing, and Luo 1989) will be employed to implement the selection task. Based on this algorithm, the iterative identification procedure can be summarised as follows

Step 1 Determine the spatial coupling terms, that is the neighbourhood sites (represented by ∇_i) of the ith site.

Step 2 Select the time lags n_y, n_u, n_e, and n_c, then the process variables involved in the identification are

$$\{y_i(t-1), \cdots, y_i(t-n_y); u_i(t), \cdots, u_i(t-n_u); \nabla_i(t), \cdots, \nabla_i(t-n_c)\} \tag{19}$$

For each process variable initialise the following parameters

- the order m of the B-spline wavelet and scaling functions used to implement the model;
- the starting resolution j_0;
- the number of resolutions s.

Step 3 Apply the forward regression orthogonal least squares algorithm to obtain the terms and parameters of the deterministic part of the CML model from a given set of candidate terms (wavelets as regressors). The selection procedure can be terminated when the norm of the residuals is less than a given tolerance. Generate the initial prediction error sequence $\{\varepsilon(t)\}$.

Step 4 Augment the initial vector of regression variables with the prediction errors and initialise a noise model. Apply the forward orthogonal estimator again to the extended model set of candidate terms to obtain the terms and parameters, and generate a fresh residual sequence. With each new fresh residual sequence, the model is updated in an iterative manner until the model parameters converge.

7

Step 5 Apply model validity tests to evaluate the model. The CML model identified using a set of data from a given spatial site can be validated on data recorded at different spatial locations by computing the model predicted output

$$\hat{\hat{y}}_i(t) = \sum_{j \le j_0, k} \theta_{j,k,0} \Psi_{j,k}^{(0)}(\hat{\hat{\mathbf{x}}}) + \sum_{j_0 \le j \le s, k, l} \theta_{j,k,l} \Psi_{j,k}^{(l)}(\hat{\hat{\mathbf{x}}}) + e_i(t) \tag{20}$$

where

$$\begin{aligned}
\hat{\hat{\mathbf{x}}} &= (\hat{\hat{y}}_i(t-1), \cdots, \hat{\hat{y}}_i(t-n_y); u_i(t), \cdots, u_i(t-n_u); \\
&\quad e_i(t-1), \cdots, e_i(t-n_e); \hat{\hat{\nabla}}_i(t), \cdots, \hat{\hat{\nabla}}_i(t-n_c))^T
\end{aligned} \tag{21}$$

The model predicted output is a much more rigorous test than the one step ahead predicted output which most authors use. If no valid models are found, then the set of candidate terms is refined in the following way

- select the resolution s to be one order higher than that currently used;
- increase the order m of the B-spline functions;
- add higher dimensional terms to the set of candidate terms.

Note that in the above identification procedure, the initial spatial neighbourhood sites of the identified site and the time lags need to be known *a priori*. In other words, the neighbourhood of the identified site, that is, the maximum possible extent of the region around that site which influences the dynamics of that site in the spatial domain and in the time domain need to be known before starting the identification. In practice, these two factors are important in determining the spatio-temporal dynamics of the underlying system. Determining which site and what time lag should be included in the model structure is therefore very important in CML identification. This problem has been studied by Guo, Mei, and Billings (2002).

5 Simulation studies

5.1 Example 1 - One-dimensional Sine-Gordon Equation

Consider the following one-dimensional Sine-Gordon equation

$$\frac{\partial^2 u(x,t)}{\partial x^2} - \frac{\partial^2 u(x,t)}{\partial t^2} = sin(u(x,t)) \tag{22}$$

Soliton solutions of the Sine-Gordon equation are very rich. Even the 1-solution soliton solution consists of two different cases - kink and anti-kink. 2-soliton solutions can be classified into several distinct cases - the collision of two kinks, the collision of two anti-kinks, the collision of

Terms	Estimates	ERR	STD
$\phi_{0,0}(y_i(t-1))$	1.4977e+000	9.4363e-001	1.0316e-001
$\phi_{0,-1}(y_i(t-1))$	-4.9863e-001	4.8554e-002	4.7081e-002
$\phi_{0,-2}(y_i(t-1))$	-2.4952e+000	7.2454e-003	1.2793e-002
$\phi_{0,-2}(y_i(t-2))$	1.9973e+000	5.0839e-004	4.2919e-003
$\phi_{0,-1}(y_i(t-2))$	9.9852e-001	6.2654e-005	7.2112e-004

Table 1: Example 1: The terms and parameters of the final CML model

a kink and an anti-kink, and a kind of bound state called a breather solution. It is very hard to identify a model, which can produce all soliton solutions. In this simulation, consider the breather solution with $p = 2$

$$u(t,x) = 4\arctan\left(\frac{p \cdot sin(\sqrt{p^2+1} \cdot t)}{\sqrt{p^2+1}\cosh(px)}\right) \tag{23}$$

The behaviour of the breather solution is actually a localized collective oscillation.

The measurement function was taken as

$$y(t,x) = u(t,x) \tag{24}$$

The reference solution was sampled at 41 equally spaced points over the spatial domain $\Omega = [-1,1], x = \{x_1, \cdots, x_{41}\}$. From each location, 500 input/output data points sampled at $\Delta t = \pi/149.82$ were generated. Note that all the data were normalised to the interval $[0,1]$. White noise with standard deviation $\sigma = 2.8176e - 004$ was superimposed on the normalised output data which are plotted in Fig.(1).

In this simulation, the initial neighbourhood was selected to be $i - 1$ and $i + 1$ in the spatial domain and $t - 1, t - 2$ in the time domain. The identification data consisted of the first 30 data points of input/output data $u_i(t), y_i(t)$ at sites $i = 11, 21$, and 31. In addition, 30 input and output data $u_i(t), y_{i-1}(t)$ and $y_{i+1}(t)$ from neighbouring locations $i - 1, i + 1$ acted as inputs during the identification. The model was identified using the forward regression orthogonal least squares algorithm with the following parameters: the order of the B-spline was 3, initial scale was 0, and the maximal resolution was 3 for all variables. The model is listed in Table (1), where ERR denotes the Error Reduction Ratio (Chen, Billings, and Luo 1989) and STD denotes the standard deviations.

The model predicted output and the model predicted error are plotted in Fig.(2) and Fig.(3), respectively. It can be observed that the prediction error increases on average as the number of prediction steps increases, and the prediction errors at the middle sites are larger than those at the end sites. These properties are mainly caused by the inherent instability of this spatio-temporal system and the effects of the noise. It is well known that the behaviour of the breather
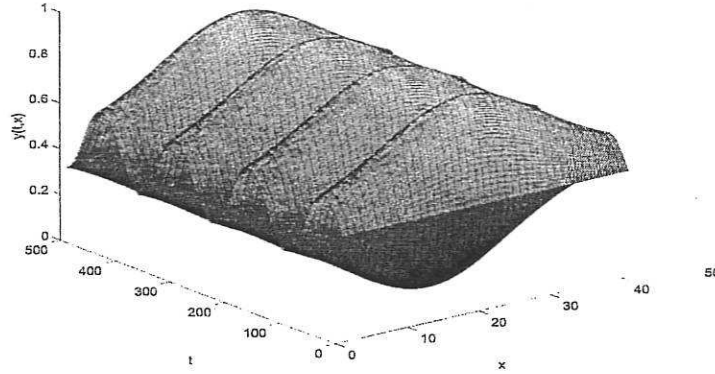
9

Figure 1: Example 1: System output

solution is actually a localized collective oscillation, which indicates the system lies in an ultimate status and any added noise could change this sustained oscillation behaviour to be stable or unstable. Furthermore the prediction error also can be caused by the maximal resolution used for the identification, which was, in this simulation, limited to be 3. The determination of the maximal resolution is actually a compromise between approximation accuracy and a parsimonious model. The simulation results also show that although there is prediction error, the deterministic patterns of the underlying dynamics have been well approximated by the identified model.

5.2 Example 2 - Predator-prey populations in ecosystems

Consider the following spatio-temporal evolution of interacting populations on a two-dimensional coupled map lattice (Sóle, Valls and Bascompte 1992, Coca and Billings 2001)

$$
\begin{aligned}
x_i(t) &= \mu x_i(t-1)(1 - x_i(t-1))\exp(-\beta y_i(t-1)) + D_1 \nabla^2 x_i(t-1) \quad (25) \\
y_i(t) &= x_i(t-1)(1 - \exp(-\beta y_i(t-1))) + D_2 \nabla^2 y_i(t-1)
\end{aligned}
$$

where $i = (i_1, i_2) \in Z^2$ and the coupling is given by a discrete diffusion operator

$$
\begin{aligned}
\nabla^2 x_{i_1,i_2} &= x_{i_1-1,i_2} + x_{i_1+1,i_2} + x_{i_1,i_2-1} + x_{i_1,i_2+1} - 4x_{i_1,i_2} \quad (26) \\
\nabla^2 y_{i_1,i_2} &= y_{i_1-1,i_2} + y_{i_1+1,i_2} + y_{i_1,i_2-1} + y_{i_1,i_2+1} - 4y_{i_1,i_2}
\end{aligned}
$$

This CML model describes the evolution of the host and parasitoid population on the lattice Z^2 in which $x_i = x_{i_1,i_2}$ and $y_i = y_{i_1,i_2}$ are the host and parasitoid population respectively. It
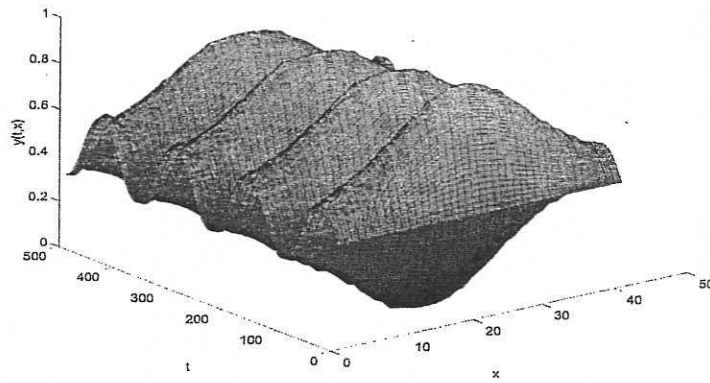
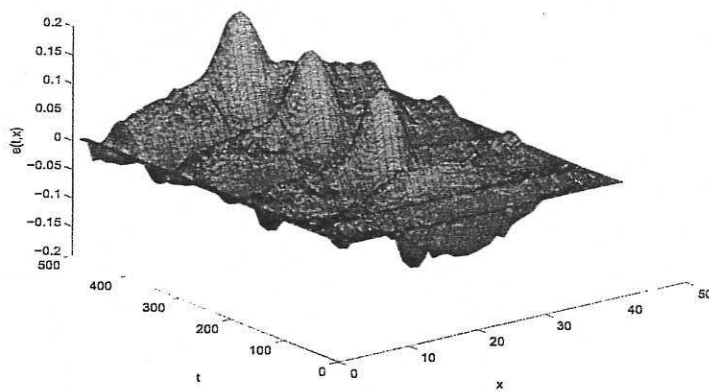10

Figure 2: Example 1: Model predicted output

Figure 3: Example 1: Model predicted error

11

has been shown (Sóle, Valls and Bascompte 1992) that this CML model is able to exhibit many interesting spatio-temporal patterns including spiral waves, chaotic and periodic dynamics under the different parameters and/or different initial conditions.

In this simulation, the measurement variables used for identification were set to be $x_i(t)$ and $y_i(t)$ for each site $i \in Z^2$ and the data used for the identification was generated by simulating the CML model (26) with $\mu = 4, \beta = 5, D_1 = 0.0001, D_2 = 0.20$ for 1000 steps over a 50×50 lattice I starting from randomly generated initial populations and periodic boundary conditions. Following Sóle, Valls and Bascompte (1992), the initial condition for which both populations were randomly generated was as follows

$$
\begin{aligned}
0.3 < \quad x_i(0) \quad < 0.4, \text{for all } i \in I \\
0.3 < \quad y_i(0) \quad < 0.4, \text{for } i \in I_0
\end{aligned} \tag{27}
$$

$I_0 = \{i_{10}, i_{20}, i_{30}, i_{40}, i_{50}\}$ being 5 randomly selected lattice sites. As stated in Sóle, Valls and Bascompte (1992), this is a situation where an initial small number of predators, which appear at random positions, leads to pattern formation. To simulate stochastic behaviour, white noise with standard deviation $\sigma = 10^{-4}$ was added to the data.

The identification was performed using the proposed method from sites $(i, j), i, j = 11, 12, \cdots, 20$ and the four nearest neighbours, namely $(i-1, j), (i+1, j), (i, j-1), (i, j+1)$ for each site (i, j). The identification data consisted of the last 10 data points out of a total of 1000 input/output data points. The initial parameters were: the order of the B-spline was 2, initial scale was 0 and the maximal resolution was 1 for all variables. The identified stochastic model is listed in Table (2)

The system and model predicted outputs are plotted in Fig.(4) and (5), which show that the identified CML model can reproduce the spatio-temporal patterns of the original system. The simulation results indicate that the prediction error increases as the number of prediction steps increase. This is because the underlying dynamics at each spatial site are 2-dimensional, each of which affects one another. This makes it more difficult to obtain a good model predicted performance compared to 1-dimensional cases.

6 Conclusions

A novel approach to the identification of CML models of stochastic spatio-temporal dynamics has been introduced. It has been demonstrated that the B-spline wavelet multiresolution approximation method provides a powerful approximation tool for the spatio-temporal dynamics of pattern formation, and that it is possible to fit CML models using only a small number of spatio-temporal locations. Simulation results were included to demonstrate that the new wavelet-based identification procedure can produce excellent final CML models. Further studies will investigate how the developed approach can be used to construct filters for noisy spatio-temporal data, and
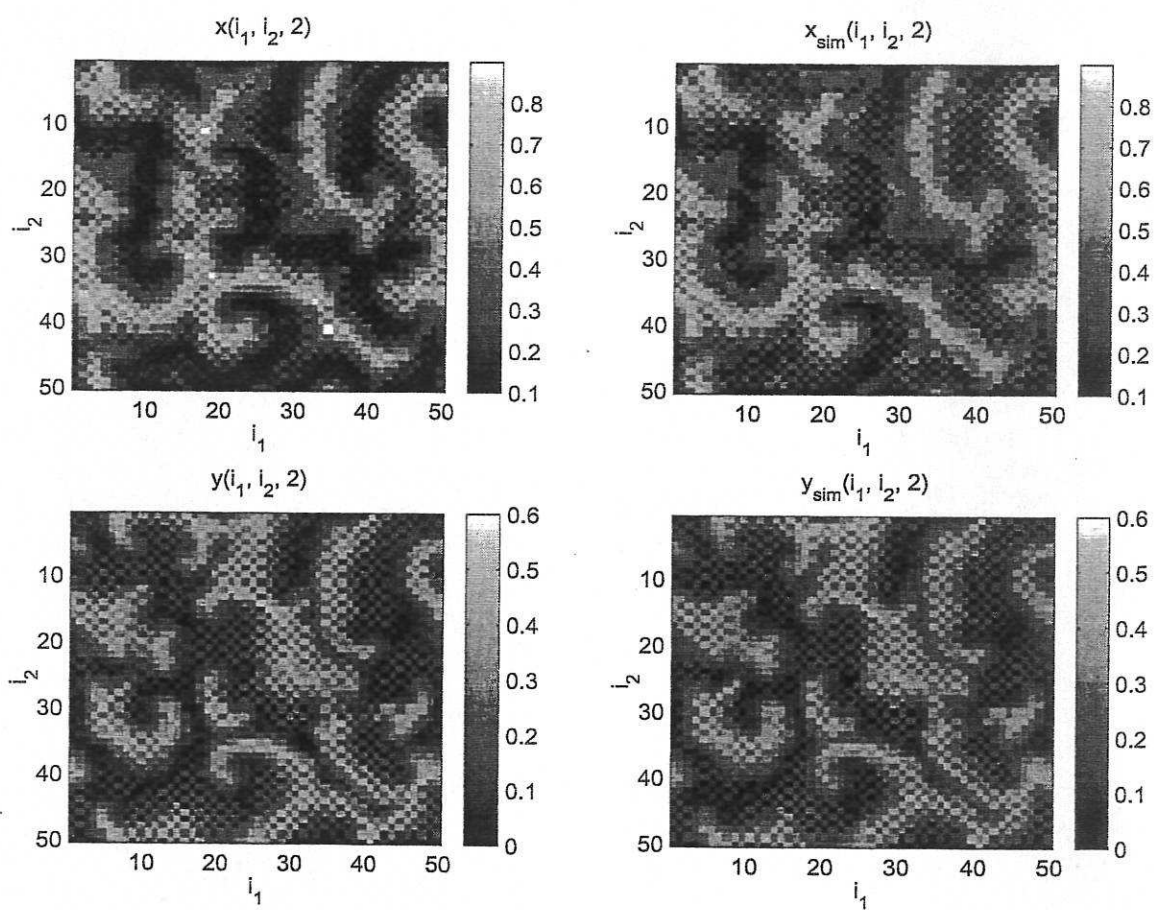
12

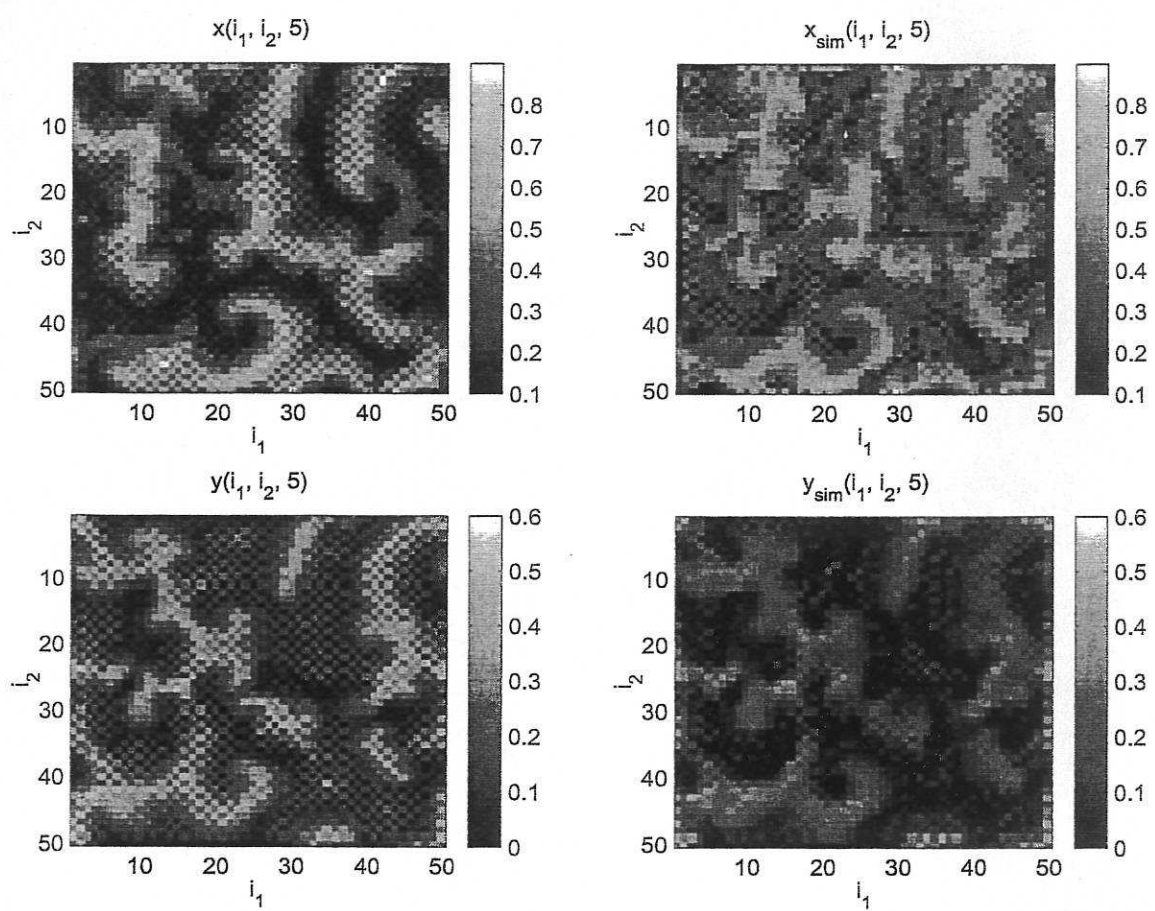Figure 4: Example 2: System and model predicted outputs at $t = 2$

Figure 5: Example 2: System and model predicted outputs at $t = 5$

Output	Terms	Estimates	ERR	STD
$x_{i_1,i_2}(t)$	$\phi_{0,-1}(x_{i_1,i_2}(t-1))\psi_{1,-1}(y_{i_1,i_2}(t-1))$	-2.5658e-002	8.5514e-001	1.4333e-001
	$\phi_{0,-2}(x_{i_1,i_2}(t-1))\psi_{1,-1}(y_{i_1,i_2}(t-1))$	-1.9924e-001	9.3175e-002	9.2298e-002
	$\psi_{1,0}(x_{i_1,i_2}(t-1))\psi_{1,-1}(y_{i_1,i_2}(t-1))$	-2.5422e-002	2.6528e-002	6.4393e-002
	$\psi_{1,0}(x_{i_1-1,i_2}(t-1))$	2.2411e-002	7.6958e-003	5.3644e-002
	$\psi_{1,0}(x_{i_1+1,i_2}(t-1))$	1.5752e-002	5.3159e-003	4.4662e-002
	$\psi_{1,0}(x_{i_1,i_2-1}(t-1))$	8.6828e-003	2.4672e-004	4.4141e-002
	$\psi_{1,0}(x_{i_1,i_2+1}(t-1))$	1.4951e-003	1.3479e-005	4.4115e-002
	$\phi_{0-2}(e_{i_1,i_2}(t-1))$	-2.6553e-002	5.8352e-004	4.3162e-002
$y_{i_1,i_2}(t)$	$\phi_{0,-2}(y_{i_1,i_2}(t-1))\phi_{0,-1}(x_{i_1,i_2}(t-1))$	7.2012e-001	7.9495e-001	1.0321e-001
	$\psi_{1,-1}(y_{i_1-1,i_2}(t-1))$	1.9684e-002	1.6051e-001	4.8437e-002
	$\psi_{1,-1}(y_{i_1+1,i_2}(t-1))$	1.8521e-002	1.4245e-002	3.9594e-002
	$\phi_{0,-2}(y_{i_1,i_2}(t-1))$	1.1662e-001	6.9306e-003	3.5658e-002
	$\psi_{1,-1}(y_{i_1,i_2}(t-1))\psi_{1,-1}(x_{i_1,i_2}(t-1))$	1.2136e-002	3.8017e-003	3.2600e-002
	$\psi_{1,-1}(y_{i_1,i_2}(t-1))\psi_{1,0}(x_{i_1,i_2}(t-1))$	-5.0963e-002	9.3897e-003	2.3538e-002
	$\psi_{1,-2}(y_{i_1,i_2-1}(t-1))$	2.3038e-002	2.0011e-003	2.1097e-002
	$\phi_{0,-2}(e_{i_1,i_2}(t-1))$	-6.4745e-002	5.4365e-004	2.0389e-002

Table 2: Example 2: The terms and parameters of the final CML model

how the amplitude and distribution of the noise perturbation affects spatio-temporal pattern formation and the identification results.

7 Acknowledgement

References

[1] Adamatzky, A., (2003) On patterns in affective media, *International Journal of Modern Physics C*, Vol. 14, No. 5.

[2] Bertram, M., Beta, C., Pollmann, M., Mikhailov, A. S., Rotermund, H. H., and Ertl, G., (2003) Pattern formation on the edge of chaos: experiments with CO oxidation on a Pt(110) surface under global delayed feedback, *Phys. Rev.*, E67, No. 3, 036208.

[3] Billings, S. A., Guo, L. Z., and Wei, H. L., (2003) Identification of spatio-temporal systems using multiresolution wavelet models, *Submitted for publications*.

[4] Billings, S. A., Wei, H. L., Mei, S. S., and Guo, L. Z., (2003) Identification of coupled map lattice models for spatio-temporal patterns using wavelets, *Submitted for publications*.

[5] Blanc-Talon, J., (1999) Effective computation of 2D coupled map lattices, *Complexity International*, Vol. 6.

[6] Chen, S., Billings, S. A., and Luo, W., (1989) Orthogonal least squares methods and their application to non-linear system identification, *Int. J. Contr.*, Vol. 50, No. 5, pp. 1873-1896.

[7] Chui, C. K. and Wang, J. Z., (1991) A general framework of compactly supported splines and wavelets, *J. Approx. Theroy*, Vol. 71, pp. 263-304.

[8] Coca, D. and Billings, S. A., (2001) Identification of coupled map lattice models of complex spatio-temporal patterns, *Phys. Lett.*, A287, pp. 65-73.

[9] Coca, D. and Billings, S. A., (2003) Analysis and reconstruction of stochastic coupled map lattice models, *Phys. Lett.*, A315, pp. 61-75.

[10] DeVore, R. A., Jawerth, B., and Popov, V., (1992) Compression of wavelet decompositions, *American Journal of Mathematics*, Vol.114, pp.737-785.

[11] Goldman, D. I., Shattuck, M. D., Sung, J. M., Swift, J. B., and Swinney, H. L., (2003) Lattice dynamics and melting of a nonequilibrium pattern, *Phys. Rev. Lett.*, Vol. 90, No. 10, 104302.

[12] Grabec, I. and Mandelj, S., (1997) Continuation of chaotic fields By RBFNN, in *Biological and Artificial Computation: From Neuroscience to Technology: Proc.*, Mira, J. et al. eds., Lecture Notes in Computer Science, Springer-Verlag, Vol. 1240, pp. 597-606.

[13] Gradisek, J., Siegert, S., Friedrich, R., and Grabec, I., (2000), Analysis of time series from stochastic processes, *Physical Review E*, Vol. 62, No. 3, pp. 3146-3155.

[14] Guo, L. Z., Mei, S. S., and Billings, S. A., (2002) Neighbourhood detection and identification of spatio-temporal dynamical systems using a coarse-to-fine approach, *Submitted for publications*.

[15] Kaneko, K. (eds.), (1993) *Coupled map lattices: theory and experiment*, World Scientific, Singapore.

[16] Köhler, P., Reinhard, K., and Huth, A., (2002) Simulating anthropogenic impacts to bird communities in tropical rain forests, *Biological Conservation*, Vol. 108, pp. 35-47.

[17] Losson, J. and Mackey, M., (1995) Evolution of probability densities in stochastic coupled map lattices, *Physical Review E*, Vol. 52, No. 2, pp. 1403-1420.

[18] Mandelj, S., Grabec, I., and Govekar, E, (2001) Statistical approach to modeling of spatiotemporal dynamics, *Int. J. Bifurcation & Chaos*, Vol. 11, No. 11, pp. 2731-2738.

[19] Marcos-Nikolaus, P., Martin-Gonzalez, J. M. and Sóle, R. V., (2002) Spatial forcasting: detecting determinism from single snapshots, *Int. J. Bifurcation and Chaos*, Vol. 12, No. 2, pp. 369-376.

[20] Parlitz, U. and Merkwirth, C., (2000) Prediction of spatiotemporal time series based on reconstructed local states, *Phys. Rev. Lett.* , Vol. 84, No. 9, pp. 2820-2823.

[21] Sóle, R. V., Valls, J. and Bascompte, J., (1992) Spiral waves, chaos and multiple attactors in lattice models of interacting populations, *Phys. Lett.*, A166, No. 2, pp. 123-128.

[22] Sweldens, W. and Piessens, R., (1994) Asymptotic error expansion of wavelet approximations of smooth function II, *Numerische Mathematik*, Vol. 68, No. 3, pp. 377-401.

[23] Tabuchi, E., Yakawa, T., Mallick, H., Inubushi, T., Kondoh, T., Ono, T., and Torii, K., (2002) Spatio-temporal dynamics of brain activated regions during drinking behaviour in rats, *Brain Research*, Vol. 951, pp. 270-279.

[24] Yanagita, T. and Kaneko, K, (1997) Modeling and characterisation of cloud dynamics, *Phys. Rev. Lett.*, Vol. 78, No. 22, pp. 4297-4300.